Structure of ultrathin Ag films on the Al(100) surface

D. S. Choi
Department of Physics, Kangwon National University, Chunchon, Kangondo 200-701, Korea

M. Kopczyk, A. Kayani, and R. J. Smith
Department of Physics, Montana State University, Bozeman, Montana 59717, USA

Guillermo Bozzolo
Ohio Aerospace Institute, 22800 Cedar Point Rd., Cleveland, Ohio 44142, USA
and NASA Glenn Research Center, Cleveland, Ohio 44135, USA
(Received 3 March 2006; published 18 September 2006)

The structure for submonolayer amounts of Ag deposited on the Al(100) surface at room temperature has been studied using low-energy electron diffraction (LEED) and low-energy ion-scattering spectroscopy (LEIS/ISS). The Ag coverage was determined using Rutherford backscattering spectroscopy. We conclude that the Ag atoms form two domains of a buckled, quasihexagonal coincident lattice structure on the Al(100) surface, having a repeat distance of 5 Al interatomic spacings in the [110] direction. The LEED pattern shows a double-domain (5×1) structure with additional intensity in those spots corresponding to a (111) close-packed hexagonal layer. The analysis of the ISS results suggests that the heights of the adsorbed Ag atoms above the Al surface are not all the same, leading to the proposed buckling model that is in agreement with recent scanning tunneling microscopy measurements. In addition, some Al atoms move from the substrate up into the Ag adlayer to form a surface alloy. Model calculations using the quantum approximate Bozzolo-Ferrante-Smith (BFS) method indicate that the hexagonal layer is energetically preferred as a result of increased nearest-neighbor coordination within the Ag layer.

DOI: 10.1103/PhysRevB.74.115407 PACS number(s): 68.55.−a, 68.35.−p, 61.18.Bn, 61.14.Hg

I. INTRODUCTION

Understanding the structure of thin metal films on a metal surface continues to be an interesting subject, both from a fundamental point of view and because of its importance to applications in thin-film and semiconductor devices. The surface structure in the early stage of metal film growth on a substrate often critically affects the film structure and physical properties of the film in subsequent layers. A particularly interesting example is the quantum well structure comprised of a thin metal film on a metal substrate.[1,2] The effect of the boundary between film and substrate is an important consideration for the resulting modification of electronic structure. Several groups have looked at Ag quantum well states on a variety of substrates, both theoretically and experimentally.[3–7] Of importance to the current investigation is the growth of thin Ag films on Al single-crystal surfaces.[7–9] The lattice constants of Al and Ag are nearly the same (4.05 Å and 4.09 Å, respectively, 1% mismatch[10]), and it is known that Al and Ag form alloys at relatively low temperatures.[11] Although the Ag-Al system has been studied extensively, very few studies have focused on the detailed structure of submonolayer deposition of Ag on Al surfaces, important to understanding the properties of quantum well states. The recent scanning tunneling microscopy (STM) studies for Ag on Al(111)[8] and Ag on Al(100)[12] have provided valuable information on the morphology for Ag films on Al surfaces, but atomic resolution with detailed atom locations have eluded detection with the STM. Thus, we are motivated to use other techniques to determine the structure of this important interface.

Most previous studies of Ag film growth on Al surfaces have dealt with Ag coverage greater than one monolayer (ML). Shivaparan[13] used high-energy ion backscattering (HEIS) and channeling, x-ray photoelectron spectroscopy (XPS), and low-energy electron diffraction (LEED) to characterize Ag films deposited on Al(100) and Al(110) surfaces at room temperature, with thickness up to 30 ML. Results show that Ag atoms occupy Al face-centered cubic (fcc) lattice sites, shadowing Al atoms in the substrate, for coverage greater than one ML on Al(100). Also, and just as importantly, Ag-Al alloy formation is present at the Ag-Al interface underlying an ordered epitaxial Ag film. Previous work by the same group also found a correlation between relative atomic sizes and the formation of alloys at the aluminum-transition metal interface.[14] Specifically, Ti atoms, with atomic radii larger than that of Al, formed an fcc epitaxial overlayer on the surface, whereas Pd, Fe, Ni, and Co, whose radii are smaller than that of Al, showed alloy formation at the metal-Al interface. Silver atoms have an atomic radius that is nearly the same as that for Al, so it is interesting to ask how this interface will evolve. Losch and Niehus[15] studied the epitaxial growth of ultrathin Ag films on Al(111) at room temperature using low-energy ion scattering (LEIS, also referred to as ISS by some authors) and Auger electron spectroscopy (AES). It was found that the Al fcc lattice structure was kept by the adsorbing Ag atoms, at least to the second layer, but indications of 3D island growth were also found. From further studies of ultrathin Ag films on Al(111), Frick and Jacobi[16] found that for substrate temperatures between 300 and 520 K, Ag grows in the Stranski-Krastanov mode on the Al(111) surface, with a 0.9% compression of the Ag

monolayer. Ag clusters three to four layers thick were also found to grow on the base Ag monolayer, causing the monolayer to undergo an additional compression of 0.3–0.5%.[17] In contrast, Karlsson *et al.*[18] found that depositing Ag on Al(111) at room temperature formed Ag_2Al in hexagonally structured clusters. The bulk Ag_2Al compound is found with a hexagonal close-packed (hcp) structure.[19] Wytenburg *et al.*[20] reported the formation of a layer of Ag_2Al at the Al-Ag interface for growth of Al films on Ag(110) and Ag(111), studied with photoemission, LEED, Auger, and work function spectroscopy. We will show that the formation of a hexagonal structure and surface alloying is directly relevant to the results reported here.

Finally, Egelhoff[21] studied the growth of thin Ag films on an Al(100) surface at room temperature, using LEED and x-ray photoemission. He observed a double-domain (5×1) LEED pattern for submonolayer Ag coverage, similar to that reported here and elsewhere,[12,13] but did not determine the Ag structure. A (1×1) LEED pattern was observed for Ag coverage of up to 30 ML.[13] The results reported here for submonolayer Ag coverage show that Ag atoms form two domains of a buckled, quasihexagonal, coincident lattice structure along one [110] direction of the Al(100) surface unit cell, with a repeat distance of 14.3 Å (5 Al interatomic spacings) in that direction. The Ag structure is commensurate with the Al(100) substrate in the other [110] direction.

II. EXPERIMENT

In the present study, the experiments were carried out in an ultrahigh vacuum chamber with a base pressure of 5×10^{-11} Torr, equipped with a 125 mm mean radius hemispherical electrostatic energy analyzer for ISS, LEED optics, a residual gas analyzer, resistively heated source for Ag deposition, and ion gun for ISS and sample cleaning. This chamber is also connected to a 2 MV van de Graaff accelerator for Rutherford backscattering analysis (RBS).[22] The diameter of the Al(100) single crystal is approximately 10 mm. Repeated Ar^+ ion sputtering and annealing were performed on the Al sample surface in the chamber until a sharp $p(1\times1)$ LEED pattern was observed for the Al(100) surface, and no sign of oxygen contamination was seen in the ISS spectra. We deposited Ag atoms using a resistively heated Ag-wrapped W wire. The RBS spectra showed the deposition rate to be 0.3 ML/min. The coverage of Ag was 0.7 ML for the ISS measurements discussed here. We define 1 ML to be 1.22×10^{15} at/cm^2, the areal density of Al atoms on the Al(100) surface. In the chamber, the pressure during Ag deposition was typically 1×10^{-8} Torr. With the ion gun in operation for ISS, the typical pressure was 2×10^{-7} Torr. When annealing the sample, a Pt-resistance thermometer measured the substrate temperature. The sample temperature during Ag film growth was near room temperature.

We used ISS in the ion detection mode,[23] along with LEED and RBS, to investigate the surface structure of Ag/Al(100). When detecting ions rather than neutrals, the high neutralization rate for the scattered ions makes ISS sensitive primarily to the structural properties in the first few atomic layers of the surface. Consequently, ISS is a powerful technique for the study of geometrical surface structures because it can be used to find bond lengths and bond directions as well as mass numbers of atoms found in the surface of a material. The He^+ ion energy used for ISS was fixed at 1 keV with a beam current ranging from 5 nA to 200 nA at the target, depending on measurement configuration and beam diameter on the sample. Ion current densities were kept as low as possible to minimize surface damage.

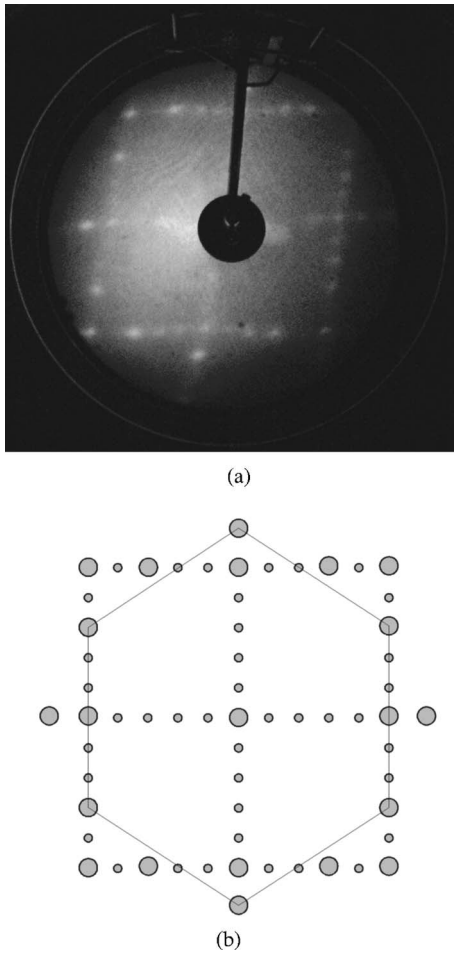

FIG. 1. (a) LEED image of 0.7 ML Ag/Al(100), showing a double-domain (5×1) pattern superimposed with a double-domain quasihexagonal pattern. (b) A schematic representation of the spot pattern in (a), with circle diameter indicating spot intensity. The solid line connects spots of near-hexagonal symmetry for one domain.

III. RESULTS

A. LEED

The LEED pattern in Fig. 1(a) shows a double-domain (5×1) structure with additional intensity in those spots corresponding to a (111) close-packed hexagonal layer. The double-domain structure is present due to the 90° symmetry of the Al(100) surface. The analysis of the ISS results presented in Sec. III B suggests that the heights of the adsorbed Ag atoms above the Al surface are not all the same, leading

to the buckling model proposed below, and in agreement with recent STM measurements for roughness of the Ag surface.[12] Egelhoff[21] reported observation of a (5×1) pattern at low Ag coverage without noting the hexagonal structure. The (5×1) LEED pattern could result at low Ag coverage if Ag atoms arranged themselves in rows, lined up with every fifth row in the Al lattice, giving an Ag coverage of about 0.2 ML, or 0.8 ML if every fifth row of Ag atoms was missing. Our RBS results indicate an Ag coverage of about 0.7 ML, and we still observe the (5×1) pattern in the LEED image. We propose instead that the root cause of the appearance of the (5×1) pattern is the quasihexagonal, coincident Ag adlayer as discussed below.

Figure 1(a) shows the LEED image obtained for 0.7 ML Ag on Al(100). Figure 1(b) is a schematic drawing for this LEED image. The drawing shows a double-domain (5×1) pattern (small circles). The (5×1) LEED pattern is interpreted as the result of repeating a surface structure for every five rows of the Al substrate lattice. The drawing also shows two domains of the quasihexagonal pattern with the larger circles along each edge segment. The solid line in Fig. 1(b) connects the spots for one domain of the quasihexagonal patterns (calculated internal angles are 118° and 121°). The larger circles at the corners and along each edge correspond to the integer order LEED spots for the substrate and overlayer. A closely related situation was reported by Bauer *et al.*[24] for Ag films on W(100), where a $p(2\times1)$ pattern was attributed to Ag atoms forming a distorted hexagonal structure on a substrate surface with square symmetry. For our experiments, the quasihexagonal structure always accompanied the (5×1) pattern for Ag coverage ranging from 0.5 ML to just over 1 ML. Neither pattern was observed separately, so we assume that islands or patches of the structure were forming at submonolayer coverage. The STM results of Veyan[12] show the formation of Ag stripes along the [110] directions of the Al surface, with the width of the stripes being 14 or 27 Å, depending on coverage. Unfortunately, the STM results do not resolve atomic structure within the stripes, so we can only speculate that the quasihexagonal structure exists within the stripes. However, the reported root-mean-square (rms) roughness of 0.6 Å is consistent with the buckling model proposed here.

B. ISS

While much about the structure of Ag/Al(100) can be inferred from the LEED pattern, a more detailed characterization of the structure is obtained from the ISS results. Following consideration of the ISS spectra, presented below, we suggest a structure model of the Ag/Al(100) surface as depicted in Fig. 2. In this figure, the small dark circles denote Al surface atoms, and the shaded circles denote Ag atoms. The different sizes of the shaded circles represent the different adsorption heights of Ag atoms on the Al substrate (the larger the circle, the greater the respective height above the Al substrate). This model suggests that the Ag atoms form rows parallel to the [110] direction and commensurate with the substrate along the vertical [110] direction of the figure, while the location of adjacent rows of Ag atoms repeat horizontally only after five Al nearest-neighbor spacings (14.3 Å) along the horizontal [110] direction, i.e., they form a 5×1 coincident lattice structure. The Ag atoms do not line up at all with the substrate along the [100] direction. A very similar situation was proposed for the (5×1) surface reconstruction of clean Ir(100), where the surface Ir atoms reconstruct into an hexagonal layer with a small uniaxial contraction to be in coincidence with every fifth row of Ir substrate atoms.[25]

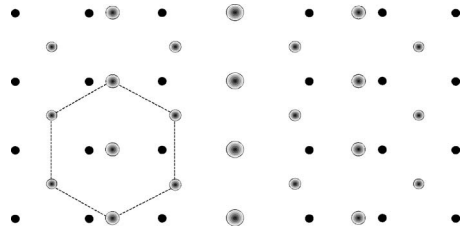

FIG. 2. Top view of the Ag/Al(100) surface inferred from the LEED pattern shown in Fig. 1. The small dark circles denote Al atoms, the larger shaded circles denote Ag atoms at different heights above the surface, and the larger circles represent atoms farther from the surface. The broken line shows the quasihexagonal unit cell.

Figure 3 shows the normalized ISS azimuthal scan curves for the Al peak height when the incoming He^+ ion beam is at an incident polar angle of 11° above the surface, for a clean Al(100) surface (solid circles), and for the

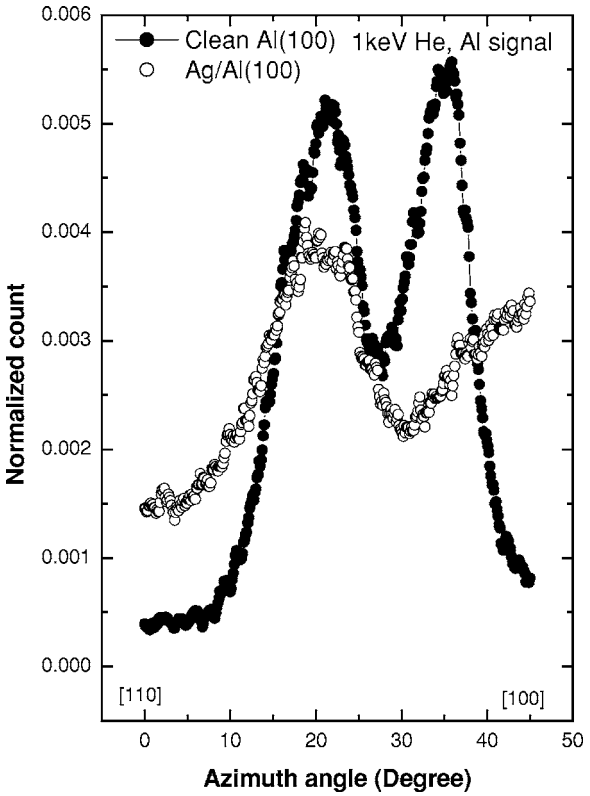

FIG. 3. Normalized ISS azimuthal scan curves, plotting point-by-point the Al ISS peak intensity for He^+ ions incident at a polar angle of 11° from grazing for the clean Al(100) surface (solid circles), and for the 0.7 ML Ag/Al(100) surface (open circles).

0.7 ML Ag/Al(100) surface (open circles). In the figure, the curves represent a point-by-point recording of Al ISS peak heights, consisting of the count rate recorded at the energy of the Al ISS peak while scanning the azimuthal angle of the incident ion beam. After Ag deposition, the intensity of the ISS peaks making up the Al signal are only about 10% of the intensity measured prior to Ag deposition. Thus, in order to make a better comparison of one signal with the other, the two signals have been normalized in Fig. 3 to have the same area under the curve, and the analysis deals primarily with the shape and locations of peaks in the respective curves.

Before Ag adsorption, the spectrum for clean Al(100) in Fig. 3 shows two deep valleys at azimuth angles of 0° ([110] direction) and 45° ([100] direction). These valleys result from the shadowing effect of target Al atoms on neighboring Al atoms as the ion beam direction is aligned with the [110] and [100] directions, respectively. The valley appearing at 26.6° is the result of Al atoms aligned with the [310] direction. After Ag adsorption, the valley in the [100] direction has been eliminated, but the valley in the [110] direction remains. Thus, in the [110] direction, Ag atoms must be lined up in rows parallel to the rows of Al atoms in the substrate below, so as not to significantly change the shadowing geometry for Al atoms. The presence of Ag atoms does result in a reduced peak-to-valley ratio for the [110] direction, as seen in Fig. 3, but a valley attributed to shadowing effects is still clearly present. In the [100] direction, however, the Ag atoms on the surface apparently do not line up in rows parallel to the substrate Al atoms but instead occupy a variety of adsorption sites, as suggested in the model of Fig. 2. Thus the shadowing of Al atoms in this direction is much more disrupted by the Ag adatoms, which appear disordered from this azimuthal perspective, and the many new Ag-Al scattering pairs for the [100] azimuth cause the valley for the [100] direction to rise much higher as compared to that for the [110] direction.

Figure 4 shows the normalized polar scan curves along the [110] direction for the clean Al(100) surface (solid circles), for 0.7 ML Ag deposition on Al(100) (open circles), and for the difference of these two curves (open diamonds). The curves represent Al ISS peak intensities, recorded while scanning the polar angle of the incident ion beam. As shown in the figure, the shapes of the two curves before and after Ag deposition are quite similar for incident angles greater than 30° and differ primarily at smaller incident angles. These data can be used as follows to infer that the Ag adatoms are distributed in a relatively flat overlayer rather than forming clusters or three-dimensional Ag islands. For a completed hexagonal overlayer in the model structure shown in Fig. 2, the Ag coverage would be 1.2 Al(100) monolayers since there is one extra row of Ag atoms for every five rows of Al atoms. However, for the measurements reported here, the coverage as determined by RBS is about 0.7 ML, which means that at least 40% of the surface consists of exposed Al(100) surface atoms. Furthermore, at larger incident angles (further from grazing incidence) the ISS scattering yield will include some contributions from scattering events in the second or third layer down from the surface. Thus, for the large incident angles, the shape of the ISS spectrum for

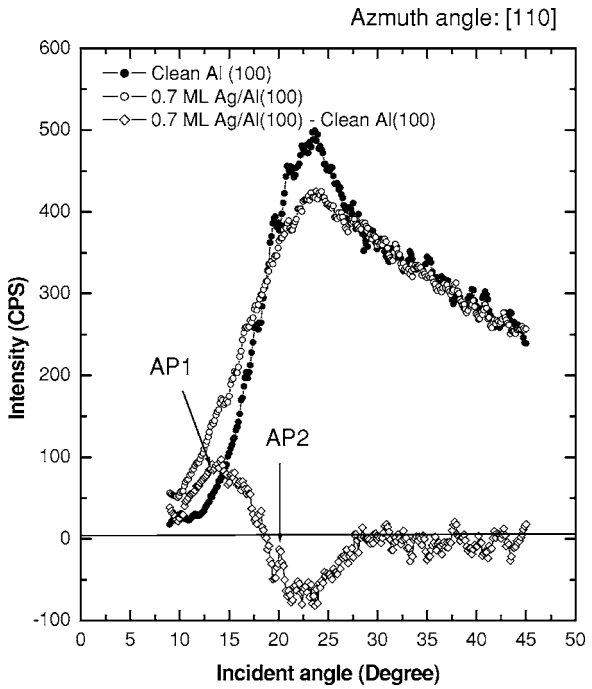

FIG. 4. Normalized ISS polar scan curves, plotting Al ISS peak intensities at an azimuth angle fixed in the [110] direction, for the clean Al(100) surface (solid circles), for the 0.7 ML Ag/Al(100) surface (open circles), and their difference (open diamonds). Peak labels are discussed in the text.

Ag/Al(100) is expected to be more similar to that for the clean Al(100) surface. On the other hand, for the smaller incident angles we do see differences in the shape of the scattering yield following Ag deposition. If the Ag atoms grow in islands rather than a flat layer, the ISS yield would not change much from that of the clean surface since the accumulation of Ag atoms in three-dimensional islands at this low Ag coverage would leave much of the clean surface exposed. We thus conclude the growth of a relatively flat Ag layer for submonolayer Ag coverage, as also seen in STM studies.[12] In contrast to these results, on Al(111) surfaces Ag growth is more three dimensional at low coverage and tends toward flat film growth for higher coverage.[8]

Referring again to Fig. 4, the difference between the two curves (before and after Ag deposition) shows enhanced scattering yield from Al atoms over a range of incident angles centered at 14.5° (AP1) and in a narrow peak located at 20.0° (AP2). Since the angular widths of typical scattering peaks for this system are on the order of 1–2° (see Fig. 5), we conclude that the broad AP1 peak represents scattering contributions originating from various Ag-Al atom pairs where one or both of the atoms have slight variations in height coordinates above the surface. For these low incident angles, this could happen if Al substrate atoms move up into the Ag layer, sitting at various heights above the Al surface plane, or causing the neighboring Ag atoms to have an increased range of heights above the surface. At these low incident angles, ions scatter primarily from Al atoms in the topmost layer and are less likely to probe Al atoms in the second or third layers. Bozzolo *et al.*[11] have argued on the basis of BFS model

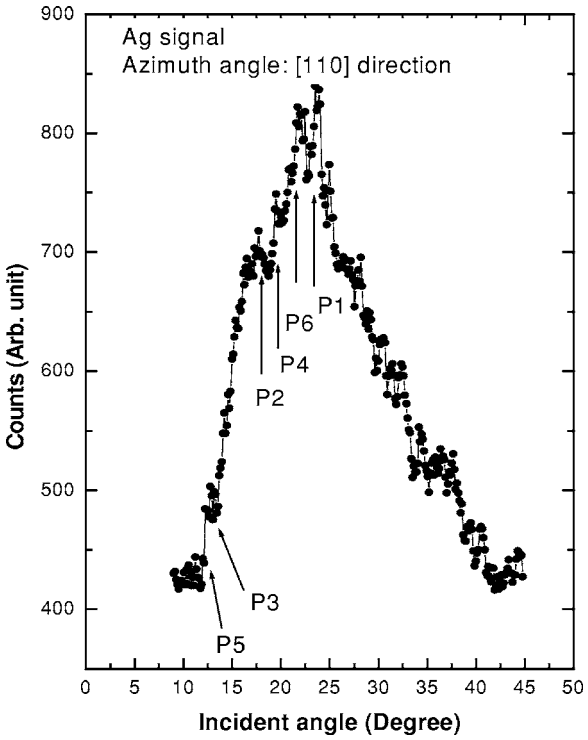

FIG. 5. ISS polar scan curve for the 0.7 ML Ag/Al(100) surface, plotting Ag ISS peak intensity at an azimuthal angle fixed in the [110] direction. Peak labels are discussed in the text.

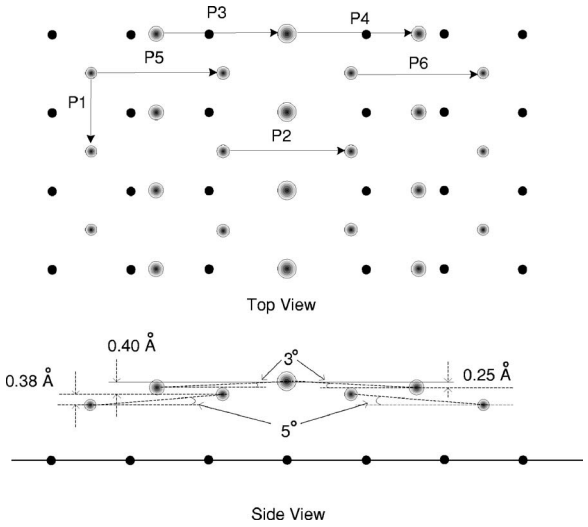

FIG. 6. Top view and side view of the proposed quasihexagonal, buckled coincident lattice model for Ag on Al(100). The small dark circles denote Al surface atoms, and the larger shaded circles denote Ag atoms. Larger circles represent Ag atoms further from the surface. The atom pairs denoted as P1,P2,…,P6 correspond to the peaks using the same nomenclature shown in Fig. 5 for He^+ ions incident from the left of the figure. The P1 atom pairs (vertical direction) are shown to represent the contribution from a second domain of this structure, rotated by 90°.

calculations that exchange of Ag and Al atoms is energetically favorable for Ag on all three low-index surfaces of Al.

Figure 5 shows the Ag ISS peak intensity, measured while scanning the polar angle of incidence for the ion beam along the [110] azimuth for the 0.7 ML Ag/Al(100) surface. This figure shows several peaks or shoulders, labeled as P1(23.5°), P2(16.5°), P3(13.5°), P4(19.5°), P5(11.5°), and P6(21.5°). The intensities of P3 and P5 are very weak because the incident angle is quite low. Many of the peaks in Fig. 5 are relatively narrow compared to the Al peaks seen in Figs. 3 and 4. We believe the overall spectrum shape in Fig. 5 is the result of superimposing a series of peaks for the atoms pairs (P1 to P6) as discussed below, each peak having a relatively narrow flux peak followed by a gradual decrease in intensity.[26] When the individual peak shapes are superimposed using the appropriate angular positions, the sharp flux peaks remain, sitting on a broad background. A smoothly varying background has also been subtracted from the original data of Fig. 5 over the region from 10° to 45°.

The following geometric analysis makes use of the shadow-cone radius for scattered ions, and the critical angle, defined to be that angle where the shadow cone made by the first Ag atom just hits the second Ag atom of the pair, calculated using the Thomas-Fermi potential. Simple geometric calculations lead to the proposed buckling model shown in Fig. 6. The small dark circles in Fig. 6 denote Al atoms in the surface plane, and the larger shaded circles denote Ag atoms. The size of the shaded circles represents the height of the Ag atoms above the Al surface, as seen in this side view. In the vertical direction of the top view in Fig. 6, the nearest-neighbor distance for Ag atoms in the hexagonal structure is 2.86 Å, commensurate with the Al substrate, leading to a critical angle of 23.5° (peak label P1). The scattering yield for this Ag-Ag pair should be large, as seen in Fig. 5, since this pair comprises the single Ag scattering contribution for one of the two domains on the surface, when the ion beam is along the vertical (commensurate) direction of Fig. 6. The P2 peak corresponds to the horizontal Ag-Ag pairs indicated in Fig. 6, with an interatomic distance of 4.8 Å, giving a calculated critical angle of 16.5° for a shadow cone radius of 1.34 Å for 1 keV He^+ ions. The other labeled peak positions differ by ±3° and ±5° from the 16.5° peak (P2), namely, at 16.5° ± 3° (P4 and P3) and 16.5° ± 5° (P6 and P5), respectively. This means that Ag-Ag atom pairs inducing these peaks are inclined vertically by ±3° and ±5° with respect to the atom pairs inducing the 16.5° peak (P2). Figure 7 shows schematically the geometrical explanations of how the peaks P5 [Fig. 7(c)] and P6 [Fig. 7(b)] are symmetrically related to the critical angle of 16.5° for P2 [Fig. 7(a)]. Such calculations lead to the proposed buckled, coincident lattice structure of Fig. 6. With the measured atomic coordinates shown in the proposed model of Fig. 6, the rms value of the Ag atom height above the surface plane is 0.4 Å. Veyan[12] reports a surface corrugation of 0.6 Å in STM images of the Ag layer on Al(100).

IV. DISCUSSION AND MODEL CALCULATIONS

It is perhaps not surprising that the Ag submonolayer structure exhibits some buckling, since this form of relaxation is one way of relieving the strain in the overlayer associated with the slight lattice mismatch (1%). The more

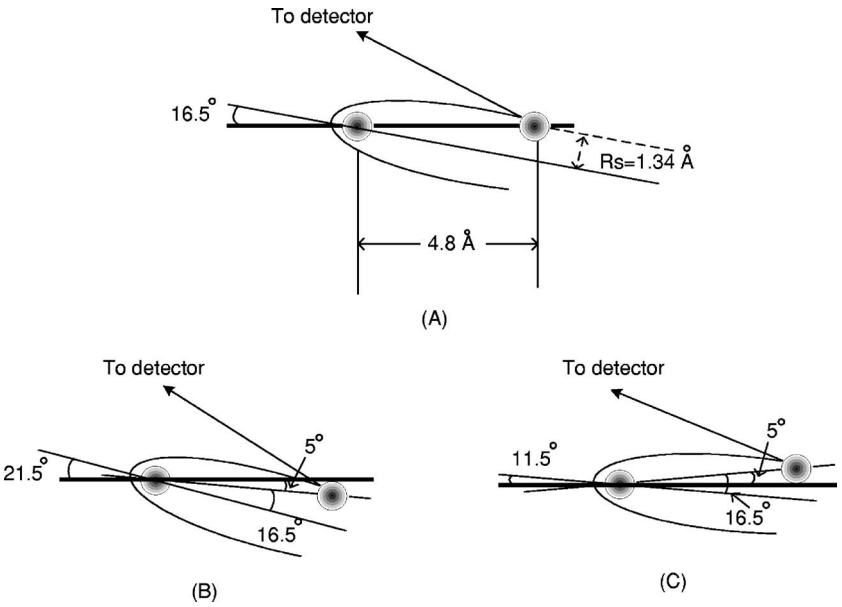

FIG. 7. (A) An Ag-Ag atom pair, whose atomic separation is 4.8 Å, induces the peak (P2) at 16.5°. (B) and (C) show that if the atom pairs are inclined by ±5° with respect to the horizontal direction, the ISS peaks will appear at 16.5° ±5° (P6 and P5 in Fig. 5).

significant surprise is the growth of the hcp structure on the square Al(100) template. The growth of this structure suggests that the Ag-Ag interatomic bond is considerably stronger than that of the Ag-Al bond, resulting in a close-packed, coincident Ag lattice structure. To further reduce the strain energy, and to maintain the best interatomic distance for Ag, the atoms on the surface form a buckled hexagonal structure. Sprunger *et al.*[4] made a similar observation in STM studies of Ag adsorption on the Cu(100) surface. For Ag-Cu(100) the lattice mismatch is much larger (~11%) compared to that for Ag-Al(100) at 1%, and is compressive in both cases. Sprunger *et al.*[4] reported a $c(10\times2)$ symmetry with a buckling structure, and also a pseudo-Ag(111) structure, similar to the results reported here. Due to the lower percentage of mismatch in the lattice parameters for Ag-Al, we expect much less buckling for Ag-Al than for Ag-Cu.

A simple modeling effort using the BFS method for alloys[27] provides an explanation for why Ag could grow on Al(100) in the hexagonal adlayer rather than as a cubic fcc (100) layer. The BFS method computes the total energy of the system by adding individual contributions, ϵ_T, from each atom. Each contribution is divided into two terms. First, a strain energy term, ϵ_S, computed as if all the neighbors of the atom were of its same species, which measures the increase in energy due to a departure from an equilibrium perfect crystal. Second, a chemical energy term, ϵ_C, computed as if all the neighbors retain their identity but occupy equilibrium sites in the lattice corresponding to the reference atom, is a measure of the attraction (negative sign) or repulsion (positive) that the reference atom exerts on each of its neighbors. Having separated structural and chemical effects, they are then reconnected by a coupling function, g, which weighs the chemical energy contribution according to the departure of the structural defect with respect to the equilibrium crystal of the reference atom. The total energy contribution to the energy of the system is then $\epsilon_T=\epsilon_S+g\epsilon_C$.

Two configurations were considered for modeling purposes: (a) a square (5×5) Ag patch on Al(100), and (b) a 5×5 diamond-shaped Ag patch on Al(111). Concentrating on the energetics of the central Ag atom in the patch and the supporting Al substrate atoms in each case [four for Al(100) and three for Al(111)], Table I shows the different BFS contributions to the total energy in each case. Monoatomic configurations (Al patches on Al substrates) would yield similar results but with $\epsilon_c=0$ and $\epsilon_S=\epsilon_T$. The central Ag atom in the square patch on Al(100) has much higher strain energy contribution (0.8277 eV) than the central Ag atom in the diamond patch on Al(111) (0.5469 eV), due to the lower coordination in the first case. As a result, the coupling function is small, $g=0.3401$ (relative to an equilibrium value $g=1$ in the monoatomic case). The chemical energy contribution for the square patch (−0.1503 eV) is lower than that in the diamond patch (−0.1390 eV), favoring the square arrangement. However, the *net* chemical energy contribution ($g\epsilon_c$) is substantially smaller (−0.051 eV) and comparable to the net chemical energy of the Ag atom in the diamond patch

TABLE I. Energy contributions (eV) of the center Ag atom to the total energy for two different configurations: (a) 5×5 square island on Al(100), and (b) 5×5 diamond-shaped island on Al(111).

Configuration	Atom	ϵ_s	g	ϵ_c	ϵ_T
(a) Cubic Ag/Al(100)	Ag atom	0.8277	0.3401	−0.1503	0.7765
	Al atom (×4)	~0	0.9985	0.1685	0.1682
(b) Diamond Ag/Al(111)	Ag atom	0.5469	0.4463	−0.1390	0.4849
	Al atom (×3)	0	1.000 0	0.1103	0.1103

(−0.0620 eV) due to the higher value of its coupling function. This, added to the much lower strain in a (111) geometry, makes the diamond patch more energetically favorable (0.4849 eV) than the square arrangement (0.7765 eV). It is clear then that the formation of a hexagonal adlayer is a strain-driven feature, as the large difference in strain between the two configurations offsets any chemical gain. As Table I also shows, any chemical gain from Ag atoms cancels out with the repulsion of the supporting Al substrate atoms.

The addition of a second Ag adlayer, however, alters this energy balance. As the additional Ag atoms increase the coordination of first-layer Ag atoms, their coupling functions approach the equilibrium value, thus increasing the attractive net chemical energy contribution with no opposing changes in the contributions from the substrate Al atoms. Therefore, Ag atoms do not need to look for alternative growth patterns to increase their coordination, which was the leading factor in the formation of a hexagonal pattern. As a result, it is expected that as the Ag coverage increases past one monolayer, the Ag overlayer will revert to the fcc symmetry. Such a structure change manifests itself in the onset of Ag-Al shadowing for high-energy backscattering/channeling measurements, as discussed elsewhere.[13]

Finally, returning to Fig. 4, we note that at low incident angles the difference curve for the polar scan of Al ISS intensity shows a relative enhancement of scattering in a broad peak centered at approximately 14.5° (AP1). We attribute this enhanced scattering to Ag-Al atom pairs of the type P2, which occurred at 16.5° for the Ag-Ag pairs in Fig. 6, but with Al atoms now replacing the second Ag atom of the pair. The width of peak AP1 could be associated with Al atoms moving up into the Ag layer but located at different heights above the Al(100) surface plane. In studies of Ag on Al(111), Kim *et al.*[9] proposed a closely related structure, with Al substrate atoms moving up into the Ag layer to occupy the center position in each unit cell of the close-packed Ag(111) layer, forming a $(\sqrt{3}\times\sqrt{3})$-*R*30° structure. Although we do not observe a $(\sqrt{3}\times\sqrt{3})$-*R*30° pattern, it is certainly consistent with our observations to have Al atoms occupying random sites in the buckled hcp structure. Even if the alloyed surface adlayer is ordered, as proposed by Kim, the Al atoms will occupy sites of various heights above the Al surface plane, leading to a broad peak like AP1. Formation of an Al-Ag surface alloy will also help to relieve strain in the overlayer. Zarkevich and Johnson[19] have studied a variety of hcp-based Ag-Al alloys and have shown that the Ag-Al interatomic distance is intermediate to that for Al-Al and Ag-Ag for the fcc (111) planes. In fact, the structure of the basal plane for Ag_2Al has a $(\sqrt{3}\times\sqrt{3})$-*R*30° structure like that proposed by Kim *et al.*[9]

The relatively sharp peak (AP2) located at 20° in the difference curve of Fig. 4 may be an artifact of forming the difference curve. Although the location of the peak is consistent with an explanation using P2 atom pairs, with the second Ag atom replaced by Al, we also note that the polar scan for the clean Al(100) surface has a slight dip at about this same angle. An absence of the same dip in the polar scan of the Ag/Al(100) surface would result in the narrow peak (AP2) near 20°.

V. SUMMARY

In summary, using LEED, RBS, and ISS, we have investigated the surface structure of 0.7 ML Ag/Al(100). We conclude that the Ag atoms form a buckled, quasihexagonal, coincident lattice structure with a repeat distance of five Al interatomic spacings along one [110] direction, resulting in the superposition of (5×1) and hexagonal LEED patterns. The heights of the adsorbed Ag atoms above the surface are not all the same, and some of the Ag atoms in the layer are replaced by Al atoms. Model BFS calculations show that the formation of the hexagonal Ag overlayer is energetically preferred as Ag adatoms increase their nearest-neighbor coordination with the close-packed structure and reduce the strain energy within the layer.

ACKNOWLEDGMENTS

One of the authors (D.S.C.) was supported by Kangwon National University while on sabbatical leave at Montana State University, and we greatly appreciate this support. We also acknowledge the technical support of Norm Williams and John Getty. This work was supported by the National Science Foundation, NSF Grant DMR 0516603.

[1] T.-C. Chiang, Surf. Sci. Rep. **39**, 181 (2000).
[2] M. Milun, P. Pervan, and D. P. Woodruff, Rep. Prog. Phys. **65**, 99 (2002).
[3] C. M. Wei and M. Y. Chou, Phys. Rev. B **68**, 125406 (2003).
[4] P. T. Sprunger, E. Laegsgaard, and F. Besenbacher, Phys. Rev. B **54**, 8163 (1996).
[5] C. Deisl, E. Bertel, M. Burgener, G. Meister, and A. Goldmann, Phys. Rev. B **72**, 155433 (2005).
[6] V. Fournee, H. R. Sharma, M. Shimoda, A. P. Tsai, B. Unal, A. R. Ross, T. A. Lograsso, and P. A. Thiel, Phys. Rev. Lett. **95**, 155504 (2005).
[7] J. F. Veyan and P. Haberle, Phys. Rev. B **72**, 073401 (2005).
[8] V. Fournee, J. Ledieu, T. Cai, and P. A. Thiel, Phys. Rev. B **67**, 155401 (2003).
[9] S. H. Kim, Jikeun Seo, Y. Shin, W. Kim, C. Y. Park, S.-J. Oh, J. M. Seo, H. G. Min, and J.-S. Kim, Phys. Rev. B **63**, 085414 (2001).
[10] N. W. Ashcroft and N. D. Mermin, *Solid State Physics* (Holt, Rinehart and Winston, New York, 1976).
[11] G. Bozzolo, J. E. Garcés, and R. J. Smith, Surf. Sci. **583**, 229 (2005), and references therein.
[12] J.-F. Veyan, Ph.D.Thesis dissertation, Universidad Tecnica Federico Santa Maria, Valparaiso (2005).
[13] N. R. Shivaparan, Ph.D.Thesis dissertation, Montana State University, (1996); R. J. Smith, C. V. Ramana, B. Choi, A. A. Saleh, N. R. Shivaparan, and V. Shutthanandan, Appl. Surf. Sci. **219**,

28 (2003).
[14] R. J. Smith, N. R. Shivaparan, V. Krasemann, V. Shutthanandan, and A. A. Saleh, J. Korean Phys. Soc. **31**, 448 (1997).
[15] A. Losch and H. Niehus, Surf. Sci. **446**, 153 (2000).
[16] B. Frick and K. Jacobi, Surf. Sci. **178**, 907 (1986).
[17] B. Frick, K. Jacobi, G. Meyer, and M. Henzler, Solid State Commun. **63**, 475 (1987).
[18] U. O. Karlsson, G. V. Hansson, and S. A. Flodström, Surf. Sci. **126**, 58 (1983).
[19] N. A. Zarkevich and D. D. Johnson, Phys. Rev. B **67**, 064104 (2003).
[20] W. J. Wytenburg, R. M. Ormerod, and R. M. Lambert, Surf. Sci. **282**, 205 (1993).
[21] W. F. Egelhoff, Jr., Appl. Surf. Sci. **11/12**, 761 (1982); J. Vac. Sci. Technol. **20**, 668 (1982).
[22] R. J. Smith, C. N. Whang, Xu Mingde, M. Worthington, C. Hennessy, M. Kim, and N. Holland, Rev. Sci. Instrum. **58**, 2284 (1987).
[23] J. Wayne Rabalais, Surf. Sci. **199/200**, 219 (1994).
[24] E. Bauer, H. Poppa, G. Todd, and P. R. Davis, J. Appl. Phys. **48**, 3773 (1977).
[25] M. A. Van Hove, R. J. Koestner, P. C. Stair, J. P. Biberian, L. L. Kesmodel, I. Bartos, and G. A. Somorjai, Surf. Sci. **103**, 189 (1981); V. Fiorentini, M. Methfessel, and M. Scheffler, Phys. Rev. Lett. **71**, 1051 (1993); G. Gilarowski, J. Mendez, and H. Niehus, Surf. Sci. **448**, 290 (2000).
[26] R. Souda, M. Aono, C. Oshima, S. Otani, and Y. Ishizawa, Surf. Sci. **128**, L236 (1983).
[27] G. Bozzolo and J. E. Garcés, in *Surface Alloy and Alloy Surfaces*, edited by D. P. Woodruff, The Chemical Physics of Solid Surfaces, Vol. 10 (Elsevier, New York, 2001).